STAG: Smart Tools and Applications in Graphics (2022)
D. Allegra, C. E. Catalano, G. Cherchi, and R. Scateni (Editors)

Poster

Multiple scattering approximation for real-time underwater spectral rendering

Nestor Monzon [1], Derya Akkaynak [2], Diego Gutierrez [1] and Adolfo Muñoz[1]

[1]Universidad de Zaragoza [2]University of Haifa

Abstract

We propose a physically-based, multispectral simulation to render underwater scenarios in real time, which also takes into account the RGB response curve of arbitrary sensors. Underwater illumination is mostly governed by multiple scattering, where light is scattered a number of times between particles before reaching the sensor. This phenomenon is therefore very low frequency and can be modeled as a function of depth and wavelength. Our approximation to multiple scattering is based on the measurable coefficient of diffuse downwelling attenuation. We show examples simulating underwater appearance under different scattering, absorption and downwelling coefficients of the Jerlov water types.

1. Introduction

Spectral rendering, where more than the three RGB wavelength bands are considered, is especially well suited for underwater scenarios. The more common atmospheric image formation model is not appropriate to simulate the appearance of the ocean, since the absorption coefficient (often more prevalent than scattering) shows great wavelength dependency [AT18]. Other phenomena like inelastic scattering [GSMA08], or the complex photoreceptors of some animals like the mantis shrimp [CBMC14], can also only be modeled by taking this wavelength dependency into account.

We present a spectral approximation to underwater illumination suitable for real-time rendering, capable of reproducing a large variety of physically-based scenarios, such as the different Jerlov water types [SM15], or different depths.

Participating media Illumination in participating media such as water is slightly more complex than surfaces, as every point along the ray contributes towards the illumination reaching the eye [GJJD09]. On non-emissive media, there are only two coefficients that model this behaviour. The scattering coefficient, σ_s (m^{-1}) is the differential probability of light being scattered per unit length travelled along the medium, while the absorption coefficient σ_a (m^{-1}) represents the probability of absorption.

Radiative Transfer Equation The radiative transfer equation (RTE), introduced by Chandrasekhar in 1950 [Cha50], describes its behaviour in a differential manner. If we focus in a light ray traveling in direction ω from point x, we can account for the derivative in radiance along the ray $\frac{dL(x_z,\omega)}{dz}$ as the amount of radiance gained, due to in-scattering, light coming from any direction scattered towards ω, minus the lost: out-scattered, or absorbed.

In-scattering More formally, the differential in radiance of in-scattered light along the ray will be $\frac{dL_{\text{in-scattering}}(x,\omega)}{dz} = \sigma_s L_i(x,\omega)$, where $L_i(x,\omega)$, in the first line, is the incident light from every direction scattered towards ω. It is defined as $L_i(x,\omega) = \int_\Omega f_s(x,\omega_i,\omega)L(x,\omega_i)\,d\omega_i$, the integral of all incident light from every direction towards point x multiplied by the phase function $f_s(x,\omega_i,\omega)$. Phase functions are the medium equivalent of BSDFs for surfaces: the ratio of light incident at point x with direction ω_i which is scattered in direction ω.

For example, in isotropic media, where light is distributed uniformly in the sphere, its value is constant, $f_s(x,\omega_i,\omega) = \frac{1}{4\pi}$. Therefore, in our case, $\frac{dL_{\text{in-scattering}}(x,\omega)}{dz} = \frac{\sigma_s}{4\pi}\int_\Omega L(x,\omega_i)\,d\omega_i$.

Extinction Usually, for convenience, out-scattering and absorption are combined into extinction, resulting in the extinction coefficient $\sigma_t = \sigma_a + \sigma_s$. This defines the differential total extinction $\frac{dL_{extinction}(x,\omega)}{dz} = -\sigma_t L(x,\omega)$, where $L(x,\omega)$ is the incident radiance which would arrive at the eye in the vacuum.

Finally, we obtain the full RTE (for non-emissive isotropic media), combining extinction and in-scattering, as we have defined them:

$$\frac{dL(x_z,\omega)}{dz} = -\sigma_t L(x_z,\omega) + \frac{\sigma_s}{4\pi}\int_\Omega L(x,\omega_i)\,d\omega_i. \qquad (1)$$

Volume rendering equation The RTE is an intuitive way to understand light transport in media, but we need to integrate it into the volume rendering equation (VRE), in order to compute the medium contribution for a ray of a given length. This integration is a well studied problem in the literature [FWKH17].

Noting $T(x_z)$ the transmittance or ratio of radiance lost between

DOI: 10.2312/stag.20221264

the sensor and point x_z, which is, by integrating the differential of the extinction, $T(x_z) = e^{-\sigma_t z}$, and L_{surf} the radiance at the surface (point x_Z), we have the general VRE for non-emissive media:

$$L(x_Z, \omega) = T(x_Z) L_{surf}(x_Z, \omega) + \int_{z=0}^{Z} T(x_z) L_i(x_z, \omega)\, dz. \qquad (2)$$

2. Multiple scattering approximation

In this work, we propose to approximate multiple scattering using the physically measurable diffuse downwelling attenuation coefficient $Kd(\lambda)$. It measures the irradiance attenuated in the water volume per meter for wavelength λ. It is usually derived from the combination of backscattering and absorption coefficients [LDC*05].

The incident irradiance (radiance from every direction) $L_i(x, \omega_i)$ from Equation (2) due to multiple scattering will be constant at every distance y from the surface, such that

$$L_i(\mathbf{x}, \omega_\mathbf{i}) = L_{ws} e^{-K_d(\lambda) y}, \qquad (3)$$

where $L_{ws}(\lambda)$ is the incident downwelling irradiance at the surface of the water body [Mob94]. Considering only the vertical variation of irradiance is a fair assumption that generalizes well, since most of the downwelling irradiance underwater comes from a natural light cone directly above, due to Snell's window, even under different sun zenith angles [SK04, HV95].

Therefore, the VRE we will evaluate for each pixel becomes $L(x_o, \omega) = T(x_s) L_{surf}(x_s, \omega) + L_{medium}(x_o, \omega)$. We already know the value of L_{surf}, from Equation (2), and we can now analytically solve the contribution from the medium as $L_{medium}(o, \omega) = \int_{z=0}^{Z} T(x_z) L_i(x_z, \omega)\, dz$. Expanding both the transmittance T and the incident radiance L_i from our approximation (Equation (3)), this results in $L_{medium}(o, \omega) = \int_{z=0}^{Z} e^{-\sigma_t z} \frac{\sigma_s}{4\pi} L_{ws} e^{-K_d y}$.

To arrive at the solution, we need to define the distance to the water surface y. If our vector ω is pointing towards the camera, this distance will be (from the ray equation $x = o + t\omega$), $y = o_y - z\omega_y$, where o_y and ω_y are the vertical coordinates of the origin and the direction vector, respectively. Finally, we can regroup all terms independent from z and solve the resulting exponential.

$$\begin{aligned} L_{medium}(o, \omega) &= \int_{z=0}^{Z} e^{-\sigma_t z} \frac{\sigma_s}{4\pi} L_{ws} e^{-K_d (o_y - z\omega_y)}\, dz \\ &= \frac{\sigma_s}{4\pi} L_{ws} e^{-K_d o_y} \int_{z=0}^{Z} e^{(Kd\omega_y - \sigma_t) z}\, dz \\ &= \frac{\sigma_s e^{-K_d o_y} L_{ws}}{4\pi (Kd\omega_y - \sigma_t)} \left(e^{(Kd\omega_y - \sigma_t) Z} - 1\right) \end{aligned} \qquad (4)$$

Evaluating this expression together with Equation (2) renders the intensity of wavelength λ, $L(\lambda)$. Given a sensor response $f(\lambda)$ that maps an intensity of wavelength λ to its RGB value, the final RGB values are mathematically the convolution of both functions over the wavelength domain: $L_{RGB} = \int_\lambda L(\lambda) f(\lambda)\, d\lambda \approx \frac{1}{n} \sum_\lambda L(\lambda) f(\lambda)$. We approximate it by discretizing it to n wavelength computations.

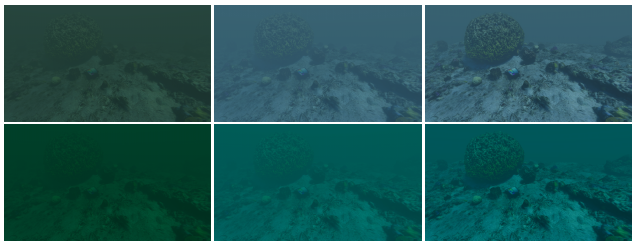

Figure 1: *Example rendered frames (at 50 fps). Each row represents the spectral response curve of different sensors, while each column illustrates a different set of spectral coefficients from Jerlov water types.*

3. Results

Figure 1 shows six example frames rendered under varying conditions. Each row corresponds to a different response curve, while each column corresponds to a different set of spectral coefficients (σ_t, σ_s and Kd), from the Jerlov water types. An additional demo video, an extended version of Figure 1, and some more HD screenshots, can be found at https://osf.io/2p3ye/?view_only=165b97d8108b45e5acc302b9b12352db.

The number of wavelengths n used in the computations can be adjusted, offering a trade-off between accuracy and frame rate. We have found $n = 8$ to be enough qualitatively (the spectral coefficients in oceans do not show a lot of high-frequency variation), while still running at 50 frames per second in 1920x1080 resolution.

4. Conclusions

Our proposed method achieves a real-time frame rate rendering spectral underwater scenes. We have integrated our method into the Unity engine High Definition Render Pipeline [Lag18] to allow the possibility to combine it with additional physically-based features in the future.

There is a trade-off between speed and physical accuracy. The proposed approximation of the complex phenomenon of multiple scattering is limited by modeling downwelling irradiance as a function of the distance to the surface. In future work, a more quantitative evaluation of the method will be carried out. Another promising step moving forward would be to integrate our work with a single scattering approximation to account for volumetric effects (such as shadows and caustics) which usually play a key role in underwater appearance.

Acknowledgements

This work was funded by the Departamento de Ciencia, Universidad y Sociedad del Conocimiento of Aragon through the research project BLINDSIGHT (ref LMP30_21), and by the European Research Council (ERC) under the EU Horizon 2020 research and innovation programme (project CHAMELEON, grant No 682080).

References

[AT18] AKKAYNAK D., TREIBITZ T.: A revised underwater image formation model. In *2018 IEEE/CVF Conference on Computer Vision and Pattern Recognition* (2018), pp. 6723–6732. doi:10.1109/CVPR.2018.00703. 1

[CBMC14] CRONIN T., BOK M., MARSHALL N., CALDWELL R.: Filtering and polychromatic vision in mantis shrimps: themes in visible and ultraviolet vision. *Philosophical Transactions of the Royal Society B: Biological Sciences 369*, 1636 (2014). doi:10.1098/rstb.2013.0032. 1

[Cha50] CHANDRASEKHAR S.: *Radiative transfer.* 1950. 1

[FWKH17] FONG J., WRENNINGE M., KULLA C., HABEL R.: Production volume rendering: Siggraph 2017 course. In *ACM SIGGRAPH 2017 Courses* (New York, NY, USA, 2017), SIGGRAPH '17, Association for Computing Machinery. URL: https://doi.org/10.1145/3084873.3084907, doi:10.1145/3084873.3084907. 1

[GJJD09] GUTIERREZ D., JENSEN H. W., JAROSZ W., DONNER C.: Scattering. In *SIGGRAPH ASIA Courses* (2009), ACM. 1

[GSMA08] GUTIERREZ D., SERON F., MUÑOZ A., ANSON O.: Visualizing underwater ocean optics. *Computer Graphics Forum (Proc. of EUROGRAPHICS) 27*, 2 (2008), 547–556. 1

[HV95] HORVÁTH G., VARJÚ D.: Underwater refraction-polarization patterns of skylight perceived by aquatic animals through snell's window of the flat water surface. *Vision Research 35*, 12 (1995), 1651–1666. URL: https://www.sciencedirect.com/science/article/pii/004269899400254J, doi:https://doi.org/10.1016/0042-6989(94)00254-J. 2

[Lag18] LAGARDE S.: The road toward unified rendering with unity's high definition render pipeline, August 2018. URL: http://advances.realtimerendering.com/s2018/index.htm. 2

[LDC*05] LEE Z.-P., DARECKI M., CARDER K. L., DAVIS C. O., STRAMSKI D., RHEA W. J.: Diffuse attenuation coefficient of downwelling irradiance: An evaluation of remote sensing methods. *Journal of Geophysical Research: Oceans 110*, C2 (2005). doi:https://doi.org/10.1029/2004JC002573. 2

[Mob94] MOBLEY C.: *Light and Water: Radiative Transfer in Natural Waters*. 01 1994. 2

[SK04] SCHECHNER Y., KARPEL N.: Clear underwater vision. In *Proceedings of the 2004 IEEE Computer Society Conference on Computer Vision and Pattern Recognition, 2004. CVPR 2004.* (2004), vol. 1, pp. I–I. doi:10.1109/CVPR.2004.1315078. 2

[SM15] SOLONENKO M. G., MOBLEY C. D.: Inherent optical properties of jerlov water types. *Appl. Opt. 54*, 17 (Jun 2015), 5392–5401. URL: https://opg.optica.org/ao/abstract.cfm?URI=ao-54-17-5392, doi:10.1364/AO.54.005392. 1